

Interpreting Behaviors and Geometric Constraints as Knowledge Graphs for Robot Manipulation Control

Chen Jiang[†], Allie Wang[†] and Martin Jagersand[†]

Abstract—In this paper, we investigate the feasibility of using knowledge graphs to interpret actions and behaviors for robot manipulation control. Equipped with an uncalibrated visual servoing controller, we propose to use robot knowledge graphs to unify behavior trees and geometric constraints, conceptualizing robot manipulation control as semantic events. The robot knowledge graphs not only preserve the advantages of behavior trees in scripting actions and behaviors, but also offer additional benefits of mapping natural interactions between concepts and events, which enable knowledgeable explanations of the manipulation contexts. Through real-world evaluations, we demonstrate the flexibility of the robot knowledge graphs to support explainable robot manipulation control.

I. INTRODUCTION

Interpreting motions by high-level descriptions, i.e. contexts (e.g. grasping a drawer handle versus opening the drawer), is a challenging problem for manipulation control. In practice, cost-effective control requires explainable task-level programming [1], [2], which coordinates operations to achieve a task. A common tool to organize task-level programming is behavior trees [3], which represent tasks as a series of behaviors and actions. However, behavior trees can overly abstract actions into high-level phrases, which do not contain the necessary low-level operation information needed for control. For example, while an action node, such as ‘grasping an apple’, clarifies the task goal, it does not specify the low-level motions required to achieve it.

On the other hand, understanding the manipulation contexts, which reflects human intentions, is crucial for selecting the right operations for the right tasks. For example, ViTa [4] constructs geometric constraints to achieve uncalibrated image-based visual servoing (UIBVS) control, where users manually associate image geometry of points and lines with specific task contexts. Further, recent advances in vision-language and foundation models [5]–[8] explore the correlation between contexts, modulated as natural language, and actions, revealing geometric features as effective embodiments of affordances that are directly usable for planning low-level motions. However, programming tasks through the classic ViTa interface is not straightforward for inexperienced users, and employing foundation models [7] is computationally expensive. The question is, how can we plan tasks with image geometry, while keeping a cost-effective and intuitive understanding of the task contexts?

In summary, we wish to preserve the interpretable nature of behavior trees in scripting actions and behaviors, while

[†]Authors are with Department of Computing Science, University of Alberta, Edmonton AB, Canada, T6G 2E8. {cjiang2, luo3, mj7}@ualberta.ca

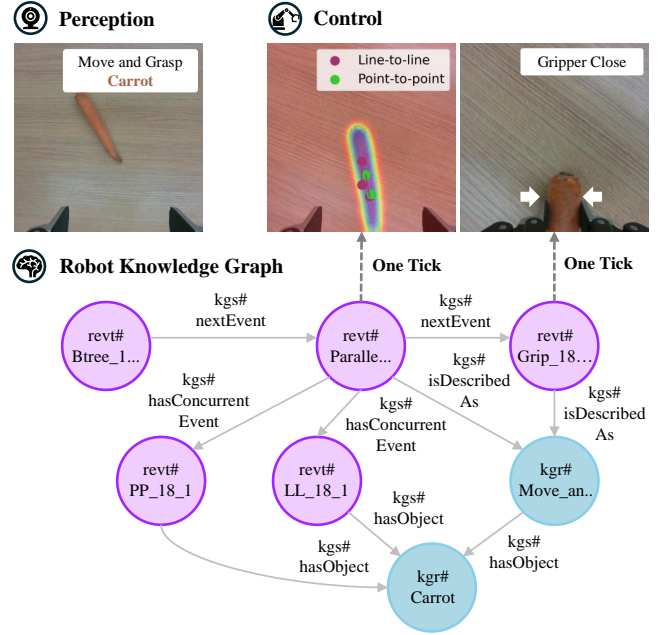


Fig. 1: An example of a robot knowledge graph to conceptualize a behavior tree and geometric constraints (a point-to-point and a line-to-line constraint) for a carrot grasping task.

establishing a clearer connection between low-level motions and high-level contexts. To this end, we propose to use knowledge graphs to achieve both goals. An example of the robot knowledge graph to relate behaviors and contexts is visualized in Figure 1. The contribution of our paper is summarized as follows:

- We present robot knowledge graphs, which unify behavior trees and geometric constraints to interpret actions and behaviors for uncalibrated visual servoing control.
- Through real-world robot manipulation experiments, we demonstrate the feasibility of using robot knowledge graphs for explainable manipulation control, while also representing the robot’s contextual knowledge of tasks.

II. RELATED WORK

A. Knowledge Graphs and Behavior Trees in Robotics

Knowledge graphs are widely studied for their applications in knowledge representation. Systems like Ahab [9] and RobotVQA [10] structured concepts for visual question answering. Similar strategies to structure concepts [11]–[16] were applied to interpret manipulation tasks in robotics.

Sequence A sequence node routes the tick from its left child to the right, returning `Success` if and only if all its children nodes return `Success`. The routing of ticks is conceptualized as a transitive relation:

$$\text{revt:Node}_i \xrightarrow{\text{kgs:nextEvent}} \text{revt:Node}_j \quad (1)$$

where Node_i and Node_j are two consecutive children of the sequence node.

Parallel A parallel node routes ticks to all its children simultaneously, returning `Success` if and only if all children nodes return `Success`. The routing of the ticks is conceptualized as a concurrent, one-to-many relation:

$$\begin{array}{c} \text{revt:Parallel} \xrightarrow{\text{kgs:hasConcurrentEvent}} \text{revt:Node}_1 \\ \vdots \\ \text{revt:Parallel} \xrightarrow{\text{kgs:hasConcurrentEvent}} \text{revt:Node}_k \end{array} \quad (2)$$

where $\{\text{Node}_1, \dots, \text{Node}_k\}$ is the set of children nodes of the parallel node.

Fallback A fallback node routes the tick from its left child to the right, returning `Success` if any child node returns `Success` and `Failure` only if all its children return `Failure`. Similar to the sequence node, The routing of ticks is conceptualized as a transitive relation:

$$\begin{array}{c} \text{revt:Node}_i \xrightarrow{\text{kgs:nextEvent}} \text{revt:Node}_j, \text{ where} \\ \text{revt:Node}_i \xrightarrow{\text{kgs:hasStatus}} \text{revt:Failure} \end{array} \quad (3)$$

where the tick is routed from the failed Node_i , to the subsequent child node Node_j .

C. Geometric Constraints as Behaviors

Instead of specifying behaviors from a linguistic perspective (e.g. approach the object, sweep table, etc), we opt for a more geometric perspective in combination with an UIBVS controller. Following [4], four types of geometric constraints are considered to describe the end-effector alignment given a set of points f :

$$\begin{aligned} \epsilon_{pp}(\mathbf{f}) &= f_2 - f_1 \\ \epsilon_{pl}(\mathbf{f}) &= f_1 \cdot f_{34} \\ \epsilon_{ll}(\mathbf{f}) &= f_1 \cdot f_{34} + f_2 \cdot f_{34} \\ \epsilon_{par}(\mathbf{f}) &= f_{12} \times f_{34} \end{aligned} \quad (4)$$

where the error signals ϵ_{pp} , ϵ_{pl} , ϵ_{ll} , and ϵ_{par} are denoted for point-to-point (p2p), point-to-line (p2l), line-to-line (l2l), and parallel-line (par) constraint, respectively. The cross product of point f_i and f_j computes a line f_{ij} . These constraints can be specified sequentially or in parallel. Given k geometric constraints, we stack the error signals as follows:

$$\epsilon = \begin{pmatrix} \epsilon_1(f_1) \\ \epsilon_2(f_2) \\ \vdots \\ \epsilon_k(f_k) \end{pmatrix} \quad (5)$$

$\{\epsilon_1, \dots, \epsilon_k\}$ are now optimized simultaneously, generating more complex, higher-level motion over time. The optimization is governed by the visuomotor control law:

$$\dot{\epsilon} = J_u(q)\dot{q} \quad (6)$$

where $\dot{\epsilon}$ is the current visual observation of the constraint ϵ , \dot{q} specifies the control input of a N degrees-of-freedom robot, and J_u is the visuomotor Jacobian.

Symbolically, we can attribute a geometric constraint as an action node of the behavior tree, regulated by `kgs:GeometricConstraintEvent` in the schema. Consequently, constraints can be simultaneously optimized, denoted by a parallel node:

$$\begin{array}{c} \text{revt:Parallel} \xrightarrow{\text{kgs:hasConcurrentEvent}} \text{revt:}\epsilon_1 \\ \vdots \\ \text{revt:Parallel} \xrightarrow{\text{kgs:hasConcurrentEvent}} \text{revt:}\epsilon_k \end{array} \quad (7)$$

Similarly, constraints can be sequentially optimized, denoted by a sequence node:

$$\text{revt:}\epsilon_1 \xrightarrow{\text{kgs:nextEvent}} \dots \xrightarrow{\text{kgs:nextEvent}} \text{revt:}\epsilon_k \quad (8)$$

D. Control with Robot Knowledge Graphs

With the robot knowledge graph, we present a pseudo-algorithm, in Algorithm 1, to enact real-world UIBVS control. In detail, the algorithm is summarized into three stages:

Algorithm 1: Enact robot control with the robot knowledge graph.

Inputs: Initial visual observation I_0 . Robot knowledge base $\{G_1, G_2, \dots\}$. Frequency $freq$.
Result: Knowledge graph G_i .
initialize an empty G_i ;
 $G_i \leftarrow \text{Query}(I_0, \{G_1, G_2, \dots\})$;
while *True* **do**
 $events \leftarrow G_i.\text{tick}()$;
 $G_i \leftarrow \text{Conceptualize}(events)$;
 $\text{sleep}(freq)$;
end
if $G_i.\text{Status} == \text{SUCCESS}$ **then**
 $\text{Union}(G_i, \{G_1, G_2, \dots\})$;
end

Specification Given the real-time visual observation of the manipulation workspace as the image frame I_0 , first, the robot analyzes the task context, which can either be specified by a user, or be determined from I_0 . Then, the robot queries a knowledge base, which is a union of graphs $\{G_1, G_2, \dots\}$, where each graph represents a successful manipulation experience, and outputs the set of behaviors and geometric constraints to perform the task.

Execution With the determined behaviors hosted inside a knowledge graph G_i , the robot ticks G_i at a fixed frequency

$freq$ (1Hz for all tasks), performing UIBVS control and completing the manipulation task. In the process, the ticking and the routing of ticks are recorded, conceptualizing the temporal transitions of behaviors as events in G_i .

Abstraction When the task is successfully completed, G_i is updated into the robot knowledge base, further enriching the robot’s common senses over a series of manipulation tasks. However, instantiating every tick leads to redundant instances of events unnecessarily populating G_i . As a post-processing step, we collapse instances of events into more abstract views before the updating step. For example, the abstraction of ticking $node_i$ is denoted as: $revt:Node_i \xrightarrow{\text{sem:hasSubEvent}} revt:Node_i^t$, where $revt:Node_i^t$ denotes the instance of the abstract event $revt:Node_i$, captured when $node_i$ is ticked at timestamp t .

IV. EXPERIMENTAL EVALUATIONS

A. Evaluation Settings

Correctness of Constraints We evaluate the explainability of knowledge graphs to determine geometric constraints from contexts. Three methods are compared:

- **Symbolic Method:** Following the proposed Algorithm 1, the symbolic method takes natural language phrases (e.g., "grasp apple") as inputs, queries a knowledge base of past successful manipulation tasks, and outputs the most relevant geometric constraints for the context.
- **CLIP-based Method:** The CLIP method constructs a zero-shot classifier using CLIP image encoder. First, initial frames of past successful manipulation tasks are encoded as reference embeddings. Then, the current visual observation is encoded. Cosine similarity is computed between the current and the reference embeddings. The geometric constraints from the most similar past task are selected as the output.
- **GPT-4o Method:** Similar to [6], prompted with the initial visual observation of the workspace and natural language phrases describing the goal of the task, GPT-4o infers the most relevant selection of geometric constraints.

From [23], 19 demonstrations of moving and grasping tasks are annotated, forming a knowledge base. The annotated knowledge base is used as the expert knowledge base for the symbolic, and CLIP-based methods. Evaluation is conducted on 12 demonstrations.

Concurrent Constraints We study the viability of scripting geometric constraints sequentially vs. concurrently. 5 trials are conducted for each of two tasks: 1) grasping a marker pen (with ϵ_{par} and ϵ_{p2p}); and 2) grasping a drink can (with ϵ_{p2l} and ϵ_{p2p}). Velocity control is employed across all trials. The average success rate and time are reported.

Real-world Robot Control We investigate the applicability of robot knowledge graphs by performing two categories of real-world manipulation tasks using everyday objects: 1) Pick-and-place, and 2) Composition. Pick-and-place tasks generally require one or two pairs of constraints to complete

the task, while composition tasks are more complex, requiring more than four behaviors or constraints. In addition, both waypoint and velocity control modes are evaluated. Waypoint control moves the end effector incrementally between waypoints as blocking actions, while velocity control continuously adjusts the end effector’s position in real time as non-blocking actions. Each control mode is allowed 3 attempts. A mode is considered successful if the robot achieves the task in at least 2 out of 3 attempts. Failing one mode results in a success rate of 50%, while failing both results in 0%. Success rate is averaged per task.

Implementation Details The robot knowledge graph is built on top of RDFlib. Querying of knowledge graphs is implemented with sparql, while the behavior trees are implemented with py_trees and ROS. For real-world robot configuration, we use an eye-in-hand Intel RealSense D405 camera and a Kinova Gen3 7-DOF arm. The saliency-based controller proposed in [6] is used for real-time visual servoing across all tasks.

B. Results on Correctness of Constraints

We report the recall of three methods for predicting geometric constraints in Table I. Overall, all methods demonstrate innate performance in predicting constraints from context, confirming the connection between manipulation contexts and image geometry.

TABLE I: Recall of methods for determining correctness of constraints.

Task Context	Method		
	Symbolic	CLIP	GPT4o [6]
Move-and-Grasp, Food	77.8%	100%	66.7%
Move-and-Grasp, Marker Pen	100%	100%	100%
Move-and-Grasp, Utility	100%	100%	100%

For the symbolic method, 1 out of 12 predictions fails for the lemon grasping task, as by design, the “lemon” concept is not present in the 19 demonstrations used to construct the knowledge base. Since the symbolic method relies solely on querying existing knowledge, it is especially vulnerable to the absence of novel concepts. This limitation could be mitigated by introducing fuzziness in contextual representation, such as canonicalizing the concept “lemon” using more knowledge sources (e.g. `dbc: Sour_fruits`). However, effective entity canonicalization is a challenging problem. In practice, combining the symbolic and CLIP-based method to incorporate both conceptual and image context can achieve more robust results.

C. Results on Concurrent Constraints

Table II reports the average success rate and execution time of concurrent versus sequential constraint optimization. Ideally, optimizing constraints concurrently yields faster execution speeds, as observed in the marker pen grasping task, where optimizing ϵ_{par} and ϵ_{p2p} in parallel is on average 42% faster than optimizing in sequence. However, concurrent optimization can be problematic. For example, in bottle

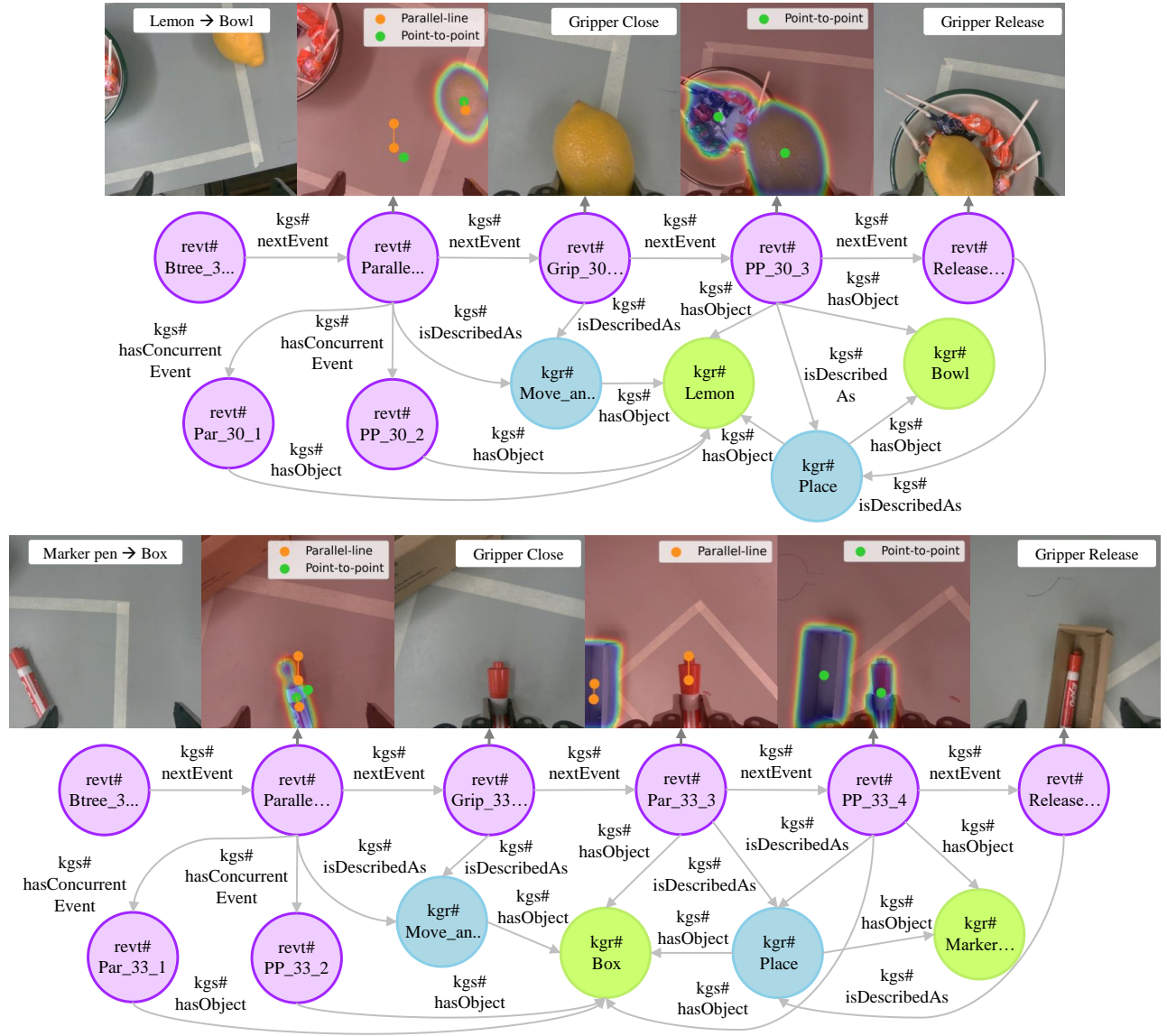


Fig. 3: Visualization of robot knowledge graphs to conceptualize pick-and-place tasks: (a) lemon \rightarrow bowl; (b) marker pen \rightarrow box. Behaviors and robot events are marked in purple, contexts in blue, and linked entities to DBpedia in green.

grasping task, the controller failed to optimize \mathcal{E}_{p2l} and \mathcal{E}_{p2p} concurrently due to rare numerical instability, resulting in dragging and eventual failure. In such cases, sequential optimization is more reliable at the expense of speed.

TABLE II: Average success rate and execution time for concurrent vs. sequential geometric constraints.

Task Context	Average Success Rate	Time
Sequence, Grasp Marker Pen	100%	24.71s
Parallel, Grasp Marker Pen	100%	17.37s
Sequence, Grasp Bottle	100%	21.61s
Parallel, Grasp Bottle	40%	23.1s

D. Results on Real-world Robot Control

Table III presents the success rates of real-world robot control across the two evaluated task categories. Overall, robot knowledge graphs retain the flexibility of behavior trees for scripting manipulation control, while effectively linking concepts and events at a detailed level. Additionally, Figure 3 visualizes the executions of two tasks, alongside the corresponding knowledge graphs.

For pick-and-place tasks, constraint specifications are flexible. For example, for pen-to-box placement, \mathcal{E}_{par} and \mathcal{E}_{p2p} can be optimized sequentially or concurrently to achieve the same placement context, which accommodates the perpendicular orientation of the rectangle box. Moreover, the optimizations perform well in both waypoint and velocity control, where the behavior trees successfully handle con-

straints as blocking or non-blocking actions respectively.

For composition tasks, repeatedly combining constraints gradually builds up the intended task goal, achieving a compositional structure with various contexts over time. Additionally, the flexibility of behavior trees allows integration with other robot behaviors. For example, in the Composition-2 task, the robot must first open the drawer to reveal the tennis ball before grasping it. Scripting such a sequence of contexts requires detailed task conceptualization, which knowledge graphs effectively represent. However, the stability of the vision model is also a crucial factor. In particular, we observe the failure of velocity control in the Composition-1 task, where obscuration over parts of the objects poses significant challenges.

TABLE III: Results with control.

Task	Context	Success Rate
Pick-and-Place	Lemon → Bowl.	100%
	Apple → Basket.	100%
	Teabag → Mug.	100%
	Marker Pen → Rectangle Box.	100%
Composition-1	2 Fruits & Candy → Basket.	50%
Composition-2	Open Drawer; Grasp Tennis Ball; Tennis Ball → Box on table.	100%

V. CONCLUSIONS

We propose to integrate behavior trees and geometric constraints into robot knowledge graphs, enabling the conceptualization and execution of real-world robot manipulation tasks. Through real-world experiments, we demonstrate the effectiveness of the robot knowledge graphs in representing manipulation contexts and events, accomplishing real-world manipulation tasks in daily living scenarios. In future work, we plan to further explore the versatility of robot knowledge graphs by scaling up the variety of daily living tasks. Additionally, automatic generation of robot knowledge graphs presents an opportunity to enhance the autonomy of the robot control, and can be valuable to explore further.

REFERENCES

- [1] M. R. Pedersen, L. Nalpanitidis, R. S. Andersen, C. Schou, S. Bøgh, V. Krüger, and O. Madsen, “Robot skills for manufacturing: From concept to industrial deployment,” *Robotics and Computer-Integrated Manufacturing*, vol. 37, pp. 282–291, 2016.
- [2] T. Sakai and T. Nagai, “Explainable autonomous robots: a survey and perspective,” *Advanced Robotics*, vol. 36, no. 5-6, pp. 219–238, 2022.
- [3] M. Colledanchise and P. Ögren, *Behavior trees in robotics and AI: An introduction*. CRC Press, 2018.
- [4] M. Gridseth, O. Ramirez, C. P. Quintero, and M. Jagersand, “Vita: Visual task specification interface for manipulation with uncalibrated visual servoing,” in *2016 IEEE International Conference on Robotics and Automation (ICRA)*. IEEE, 2016, pp. 3434–3440.
- [5] S. Levine, C. Finn, T. Darrell, and P. Abbeel, “End-to-end training of deep visuomotor policies,” *The Journal of Machine Learning Research*, vol. 17, no. 1, pp. 1334–1373, 2016.
- [6] C. Jiang, A. Luo, and M. Jagersand, “Robot manipulation in salient vision through referring image segmentation and geometric constraints,” *arXiv preprint arXiv:2409.11518*, 2024.
- [7] F. Liu, K. Fang, P. Abbeel, and S. Levine, “Moka: Open-vocabulary robotic manipulation through mark-based visual prompting,” in *First Workshop on Vision-Language Models for Navigation and Manipulation at ICRA 2024*, 2024.

- [8] W. Tang, J.-H. Pan, Y.-H. Liu, M. Tomizuka, L. E. Li, C.-W. Fu, and M. Ding, “Geomaniip: Geometric constraints as general interfaces for robot manipulation,” *arXiv preprint arXiv:2501.09783*, 2025.
- [9] P. Wang, Q. Wu, C. Shen, A. v. d. Hengel, and A. Dick, “Explicit knowledge-based reasoning for visual question answering,” *arXiv preprint arXiv:1511.02570*, 2015.
- [10] F. K. Kenfack, F. A. Siddiky, F. Balint-Benczedi, and M. Beetz, “Robotvqa—a scene-graph-and deep-learning-based visual question answering system for robot manipulation,” in *2020 IEEE/RSJ International Conference on Intelligent Robots and Systems (IROS)*. IEEE, 2020, pp. 9667–9674.
- [11] A. Saxena, A. Jain, O. Sener, A. Jami, D. K. Misra, and H. S. Koppala, “Robobrain: Large-scale knowledge engine for robots,” *arXiv preprint arXiv:1412.0691*, 2014.
- [12] C. Jiang, M. Dehghan, and M. Jagersand, “Understanding contexts inside robot and human manipulation tasks through vision-language model and ontology system in video streams,” in *2020 IEEE/RSJ International Conference on Intelligent Robots and Systems (IROS)*. IEEE, 2020, pp. 8366–8372.
- [13] M. Sukhwani, V. Duggal, and S. Zahrai, “Dynamic knowledge graphs as semantic memory model for industrial robots,” *arXiv preprint arXiv:2101.01099*, 2021.
- [14] A. Daruna, D. Das, and S. Chernova, “Explainable knowledge graph embedding: Inference reconciliation for knowledge inferences supporting robot actions,” in *2022 IEEE/RSJ International Conference on Intelligent Robots and Systems (IROS)*. IEEE, 2022, pp. 1008–1015.
- [15] R. Miao, Q. Jia, F. Sun, G. Chen, H. Huang, and S. Miao, “Semantic representation of robot manipulation with knowledge graph,” *Entropy*, vol. 25, no. 4, p. 657, 2023.
- [16] M. S. Sakib and Y. Sun, “From cooking recipes to robot task trees—improving planning correctness and task efficiency by leveraging llms with a knowledge network,” in *2024 IEEE International Conference on Robotics and Automation (ICRA)*. IEEE, 2024, pp. 12 704–12 711.
- [17] Y. Cao and C. G. Lee, “Behavior-tree embeddings for robot task-level knowledge,” in *2022 IEEE/RSJ International Conference on Intelligent Robots and Systems (IROS)*. IEEE, 2022, pp. 12 074–12 080.
- [18] D. C. Domínguez, M. Iannotta, J. A. Stork, E. Schaffernicht, and T. Stoyanov, “A stack-of-tasks approach combined with behavior trees: A new framework for robot control,” *IEEE Robotics and Automation Letters*, vol. 7, no. 4, pp. 12 110–12 117, 2022.
- [19] M. Iovino, J. Förster, P. Falco, J. J. Chung, R. Siegwart, and C. Smith, “On the programming effort required to generate behavior trees and finite state machines for robotic applications,” in *2023 IEEE International Conference on Robotics and Automation (ICRA)*. IEEE, 2023, pp. 5807–5813.
- [20] J. Liang, Y. Chang, Q. Wang, Y. Wang, and X. Yi, “Diagbt: An explainable and evolvable robot control framework using dialogue generative behavior trees,” in *2024 IEEE/RSJ International Conference on Intelligent Robots and Systems (IROS)*. IEEE, 2024, pp. 7056–7062.
- [21] X. Chen, Y. Cai, Y. Mao, M. Li, W. Yang, W. Xu, and J. Wang, “Integrating intent understanding and optimal behavior planning for behavior tree generation from human instructions,” *arXiv preprint arXiv:2405.07474*, 2024.
- [22] H. Zhou, Y. Lin, L. Yan, J. Zhu, and H. Min, “Llm-bt: Performing robotic adaptive tasks based on large language models and behavior trees,” in *2024 IEEE International Conference on Robotics and Automation (ICRA)*. IEEE, 2024, pp. 16 655–16 661.
- [23] C. Jiang, Y. Yang, and M. Jagersand, “Clipunetr: Assisting human-robot interface for uncalibrated visual servoing control with clip-driven referring expression segmentation,” in *2024 IEEE International Conference on Robotics and Automation (ICRA)*. IEEE, 2024, pp. 6620–6626.
- [24] J. Gao, Z. Tao, N. Jaquier, and T. Asfour, “K-vil: Keypoints-based visual imitation learning,” *arXiv preprint arXiv:2209.03277*, 2022.
- [25] J. Jin and M. Jagersand, “Generalizable task representation learning from human demonstration videos: a geometric approach,” in *2022 International Conference on Robotics and Automation (ICRA)*. IEEE, 2022, pp. 2504–2510.
- [26] S. Guan, X. Cheng, L. Bai, F. Zhang, Z. Li, Y. Zeng, X. Jin, and J. Guo, “What is event knowledge graph: A survey,” *IEEE Transactions on Knowledge and Data Engineering*, 2022.
- [27] W. R. Van Hage, V. Malaisé, R. Segers, L. Hollink, and G. Schreiber, “Design and use of the simple event model (sem),” *Journal of Web Semantics*, vol. 9, no. 2, pp. 128–136, 2011.